

Effects of Loss of Classical Estrogen Response Element Signaling on Bone in Male Mice

Farhan A. Syed, Daniel G. Fraser, Thomas C. Spelsberg, Clifford J. Rosen, Andree Krust, Pierre Chambon, J. Larry Jameson, and Sundeep Khosla

Endocrine Research Unit (F.A.S., D.G.F., S.K.) and Department of Biochemistry and Molecular Biology (T.C.S.), Mayo Clinic College of Medicine, Rochester, Minnesota 55905; The Jackson Laboratory (C.J.R.), Bar Harbor, Maine 04609; Institut de Genetique et de Biologie Moleculaire et Cellulaire (A.K., P.C.), Institut Clinique de la Souris, Centre National de la Recherche Scientifique/Institut National de la Santé et de la Recherche Médicale/Université Louis Pasteur, Collège de France, 75231 Illkirch Cedex, France; and Department of Endocrinology (J.L.J.), Northwestern University, Chicago, Illinois 60208

The role of estrogen signaling in the male skeleton via estrogen receptor (ER)- α is now well established. ER α can elicit responses through either classical estrogen response elements (ERE) pathways or nonclassical, non-ERE pathways. In the present study, we examined the effects of either the attenuation or loss of classical ER α signaling on the murine male skeleton. To accomplish this, we crossed male mice heterozygous for a knock-in mutation [nonclassical ER α knock-in (NERKI)], which abolishes the ERE-mediated pathway with female heterozygous ER α knockout mice (ER $\alpha^{+/-}$) and studied the F1 generation ER $\alpha^{+/+}$, ER $\alpha^{+/-}$, ER $\alpha^{+/NERKI}$, and ER $\alpha^{-/NERKI}$ male progeny longitudinally using bone density and histomorphometry. The only ER α allele present in ER $\alpha^{-/NERKI}$ mice is incapable of classical ERE-mediated signaling, whereas the heterozygous ER $\alpha^{+/NERKI}$ mice have both one intact ER α and one NERKI allele. As compared with ER $\alpha^{+/+}$ littermates (n =

10/genotype), male ER $\alpha^{+/NERKI}$ and ER $\alpha^{-/NERKI}$ mice displayed axial and appendicular skeletal osteopenia at 6, 12, 20, and 25 wk of age, as demonstrated by significant reductions in total bone mineral density (BMD) at representative sites (areal BMD by dual-energy x-ray absorptiometry at the lumbar vertebrae and femur and volumetric BMD by peripheral quantitative computed tomography at the tibia; $P < 0.05$ – 0.001 vs. ER $\alpha^{+/+}$). The observed osteopenia in these mice was evident in both trabecular and cortical bone compartments. However, these decreases were more severe in mice lacking classical ER α signaling (ER $\alpha^{-/NERKI}$ mice), compared with mice in which one wild-type ER α allele was present (ER $\alpha^{+/NERKI}$ mice). Collectively, these data demonstrate that classical ER α signaling is crucial for the development of the murine male skeleton. (*Endocrinology* 148: 1902–1910, 2007)

THE MALE SKELETON was traditionally believed to be maintained principally by androgens, but the description by Smith *et al.* (1) of a 28-yr-old male with homozygous inactivating mutations of the estrogen receptor (ER)- α gene initially challenged this premise. Since then, severe osteopenia and unfused epiphyses have also been reported in young men with mutations in the gene for the enzyme aromatase, which converts androgens to estrogens (2, 3). In one of these subjects, estrogen therapy corrected the abnormalities by increasing bone mass and leading to epiphyseal closure (3). In agreement with the human data, mice with knockout of the aromatase gene had reduced trabecular bone volume and thickness (4) and increased bone remodeling (5). It has also recently been reported that overexpression of the human

P450 aromatase enzyme results in increased trabecular bone mineral density (BMD) and decreased longitudinal growth rate and bone formation rates in young and old male mice (6). Such studies have unequivocally established the importance of estrogen action on the murine male skeleton.

The actions of estrogen are mediated by two related receptors, ER α and ER β (7). Studies using knockout mice for ER α , ER β , or both have provided considerable insight into the role of these receptors in the skeleton (8–10). Using ER $\alpha^{-/-}$, ER $\beta^{-/-}$, and ER $\alpha^{-/-}$ ER $\beta^{-/-}$ mice, Vidal *et al.* (8) were the first to demonstrate that ER α , and not ER β , mediated the important effects of estrogen on the skeleton of male mice. Consistent with this, Sims *et al.* (9) used independently generated ER α knockout mice (11) and showed that loss of ER β in male mice did not have any effect on bone, whereas loss of ER α led to decreases in cortical density and thickness. Furthermore, the same group also demonstrated that estradiol was totally ineffective in preventing orchidectomy-induced bone loss in ER $\alpha^{-/-}$ male mice, establishing the crucial role that ER α played in the male skeleton (10).

Estrogen modulates transcription in its target tissues through either of its receptors using a number of signaling pathways. Based on our current understanding of estrogen action, two pathways have been defined. The classical pathway involves direct DNA binding of the liganded receptor to estrogen response elements (EREs) (12) in the promoter regions of responsive genes such as those of prolactin (13),

First Published Online January 4, 2007

Abbreviations: aBMD, areal BMD; AP-1, activator protein-1; BFR, bone formation rate; BMD, bone mineral density; BSI, bone strength index; BV, bone volume; CSI, compressive strength index; CT, computed tomography; μ CT, micro-CT; CV, coefficient of variation; DXA, dual-energy x-ray absorptiometry; E₂, estradiol; ER, estrogen receptor; ERE, estrogen response element; LID-ALSKO, both liver IGF-I knockout and acid labile subunit; MAR, mineral apposition rate; NERKI, nonclassical ER α knock-in; ovx, ovariectomy; pQCT, peripheral quantitative CT; T, testosterone; TbN, trabecular number; TV, tissue volume; vBMD, volumetric BMD.

Endocrinology is published monthly by The Endocrine Society (<http://www.endo-society.org>), the foremost professional society serving the endocrine community.

progesterone receptor (14), and *c-fos* (15). The alternate, nonclassical pathway involves the indirect modulation of transcription by the interaction of the ER with components of other transcription complexes via protein-protein interactions. For example, ER can interact with *c-fos* and *c-jun* of the activator protein-1 (AP-1) transcription complex, up-regulating AP-1-responsive genes such as collagenase (16) and IGF-I (17). Down-regulation of the IL-6 gene transcription by ER via interactions with the nuclear factor- κ B complex has also been reported (18). In addition, estrogen can signal through membrane receptors involving MAPK signaling (19); indeed, such a nongenotropic pathway has been suggested to be sufficient for the bone anabolic actions of estrogen with no role for classical estrogen actions (20).

Although classical and nonclassical pathways of estrogen have been studied extensively *in vitro* (13, 14, 16, 21), it has not been possible, until recently, to dissect the relative contributions of these pathways *in vivo* in any tissue, including bone. The generation, by Jakacka *et al.* (22), of mice which have two substitution mutations (E207A/G208A) in the first zinc finger of the DNA binding domain in one of the ER α alleles provided a unique opportunity to address this issue. *In vitro*, this mutant receptor fails to activate ERE reporter constructs but has intact transcriptional activity for AP-1 reporter constructs and its ability to interact with *c-jun* in a mammalian cell, two-hybrid assay is unaffected (23). Heterozygote female nonclassical ER α knock-in (NERKI) mice are infertile and display pronounced reproductive defects (22), suggesting that the balance between classical and nonclassical estrogen signaling has important biological consequences *in vivo*. We recently generated female ER $\alpha^{-/NERKI}$ mice that completely lack classical ER α signaling but have intact signaling via the nonclassical ER α pathway and have characterized the skeletal phenotype and responses to ovariectomy (ovx) and estrogen replacement in these mice (24). In the female mice, we observed severe cortical osteopenia and paradoxical responses to ovx and estrogen replacement in cortical bone in ER $\alpha^{-/NERKI}$ but not ER $\alpha^{+/NERKI}$ mice. The changes observed in the ER $\alpha^{-/NERKI}$ mice were also distinct from those in the complete ER α knockout female mice, suggesting unique actions of the NERKI allele on bone. Furthermore, the basal skeletal deficits were present in cortical but not trabecular bone, although the response to estrogen after ovx was significantly attenuated in trabecular bone in both the ER $\alpha^{+/NERKI}$ and ER $\alpha^{-/NERKI}$ mice. This study confirmed that there was, indeed, a balance between the two estrogen signaling pathways and that the alteration of this balance had important skeletal consequences, at least in female mice (24).

As discussed earlier, because estrogen plays such an important role in the male skeleton, it was of interest to assess the consequences of the alteration of the balance between the classical and nonclassical estrogen signaling pathways on bone in male mice. Thus, in this study we define the skeletal phenotype of male ER $\alpha^{+/NERKI}$ and ER $\alpha^{-/NERKI}$ mice and also place the changes observed in the male mice in the context of the alterations we previously observed in the female ER $\alpha^{-/NERKI}$ mice.

Materials and Methods

Generation, breeding, and care of animals

Heterozygote NERKI male (ER $\alpha^{+/NERKI}$) mice (22) in a 129SVJ background were crossed with heterozygote ER $\alpha^{+/-}$ female mice on a C57BL/6 background (11). The resultant F1 ER $\alpha^{+/+}$, ER $\alpha^{+/-}$, ER $\alpha^{+/NERKI}$, and ER $\alpha^{-/NERKI}$ male progeny on identical 50:50 C57BL/6:129SVJ backgrounds were studied. All relevant comparisons were made within these four groups. The animals were housed in a temperature-controlled room (22 \pm 2 C) with a daily 12-h light, 12-h dark schedule. During the study, animals had free access to water and were fed a soy-free casein-based diet (AIN 93M; Dyets, Bethlehem, PA). Pups were genotyped at 4–5 wk of age and at the completion of the study by PCR as described previously (11, 22). The Institutional Animal Care and Use Committee approved all animal protocols.

Study design

Male ER $\alpha^{+/+}$, ER $\alpha^{+/-}$, ER $\alpha^{+/NERKI}$, and ER $\alpha^{-/NERKI}$ mice were initially scanned at 6 wk of age by dual-energy x-ray absorptiometry (DXA) at the femur and spine to obtain areal BMDs (aBMDs) and by peripheral quantitative computed tomography (pQCT) at the tibial metaphysis and diaphysis to obtain volumetric BMDs (vBMDs) and geometric parameters (n = 10/ genotype). Body weights were taken using a weighing scale, and right femur lengths were measured from the pQCT scout view images. The same mice were then rescanned at the same sites and for the same parameters at 12, 20, and 25 wk of age. The mice received calcein injections (10 mg/kg) at wk 22 and tetracycline injections at wk 24. At wk 26, the animals were bled by cardiac puncture and killed by inhalation of CO₂, and lumbar spines (L1-L4), tibias, and femurs were excised for histomorphometric analysis from ER $\alpha^{+/+}$, ER $\alpha^{+/NERKI}$, and ER $\alpha^{-/NERKI}$ mice.

BMD measurements

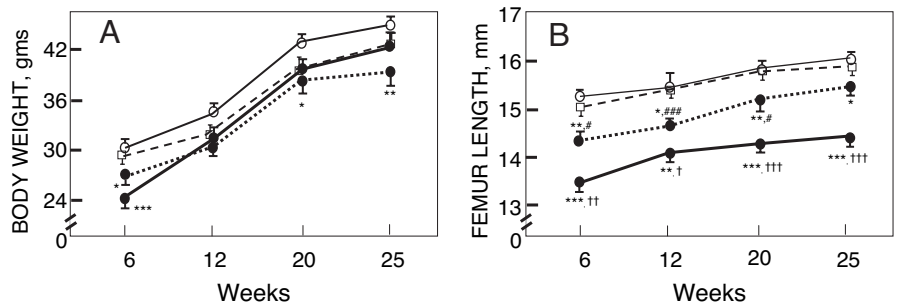
The mice were anesthetized with avertin (2, 2, 2 tri-bromo-ethanol, 720 mg/kg, ip). DXA and pQCT measurements were essentially as described earlier (24). DXA measurements were done using a Lunar PIXImus densitometer (software version 1.44.005; Lunar Corp., Madison, WI). Calibration of the machine was performed before scanning the mice using the hydroxyl apatite phantom provided by the manufacturer. Mice were then placed in a prone position on an animal tray and the whole body was scanned. After scanning, the lumbar vertebrae (L1-L4) and femur were analyzed by defining regions of interest around these bones. In repeatedly repositioned and scanned mice, the coefficients of variation (CVs) for the lumbar and femoral aBMD were 7.9 and 6.3%, respectively. For the pQCT measurements, similar to the DXA measurements, daily calibration was performed before scanning mice using the hydroxyl apatite phantom provided by the manufacturer. Anesthetized mice were then placed in a supine position on a gantry and scanned using a Stratec XCT Research SA Plus machine and analyzed with software version 5.40 (Norland Medical Systems, Fort Atkinson, WI). The mice were positioned in a manner that allowed the total length of the femur and tibia to be visible on the scout view. The scout view speed was set at 15.0 mm/sec with a slide distance of 0.5 mm. On completion of the scout view scan, the reference lines for the computed tomography (CT) scans were set at the proximal-most point of the tibia. Two slices were measured at 1.9 mm and approximately 9 mm (at the tibial-fibular synopsis) from the proximal end of the tibia to account for the metaphyseal and diaphyseal regions, respectively. The CT speed was set at 3 mm/sec, the voxel size at 100 μ m, and the slice thickness was 0.5 mm. The threshold for trabecular bone was set at 480 mg/cm³ and the cortical bone threshold was set at 710 mg/cm³. The same thresholds and settings were used on repeated scans and at all time points. After scanning, the slices were analyzed using peelmode 2, cortmode 1, and contour mode 1 to evaluate trabecular and cortical parameters. The CVs for total, trabecular, and cortical vBMDs at the metaphysis were 1.2, 2.4, and 1.9%, respectively. The CV for cortical bone at the diaphysis was 1.4%.

Calculation of biomechanical indices from pQCT data

Indices of bone structural strength and bending/torsional strength were either derived or calculated from the pQCT data obtained at all the time points. At the tibial metaphysis, the compressive strength index (CSI) was computed as the square of the integral vBMD multiplied by

ER ^{+/+} —○— ER ^{+/-} -□- ER ^{+/NERKI} ...●... ER ^{-/NERKI} —●—

FIG. 1. Total body weights (A) and femur lengths (B) ($n = 10/\text{genotype}$ per time point). *, $P < 0.05$, **, $P < 0.01$, ***, $P < 0.001$ vs. $ER\alpha^{+/+}$ mice; #, $P < 0.05$, ###, $P < 0.001$ vs. $ER\alpha^{+/-}$ mice; †, $P < 0.05$, ††, $P < 0.01$, †††, $P < 0.001$ vs. $ER\alpha^{+/NERKI}$ mice.



the bone cross-sectional area. At the tibial diaphysis, the bone strength index (BSI) (a measure of bending strength) was calculated by multiplying the cortical vBMD at this site with the cortical areal cross-sectional moment of inertia. In addition, we also report the cortical cross-sectional moment of inertia and cortical moment of resistance for the cortical shell at the tibial metaphysis and diaphysis as an index of torsional strength.

Cortical and trabecular bone histomorphometry

The femurs and lumbar spines (L1-L4) were processed for histomorphometry as previously described (24, 25). For the calculation of mineral apposition rates (MARs) at the periosteal and endosteal cortical bone surfaces of the femur diaphysis, 150- μm -thick cross-sections at the center of the bone toward the distal side were cut using a diamond edge saw (Isomet; Buehler, Lake Bluff, IL). These unstained sections were then ground on a roughened glass surface to a thickness of 25 μm for visualization of flouochrome labels. The MAR was calculated by dividing the width between the first calcein label and either the periosteal or endosteal bone surface and the time between the first calcein label and the day the animals were killed (28 d). This was done because the tetracycline label given on wk 24 was not very clearly distinguishable from the bone surface. To assess trabecular bone parameters, the dehydrated lumbar spines were embedded in methylmethacrylate, sectioned, and either unstained to determine MARs and bone formation rates (BFRs) as described above or stained with the Goldner's stain to calculate bone volumes and eroded surfaces. Osteoblast number was defined as the number of osteoblasts per millimeter of cancellous perimeter and the osteoclast number as the number of multinucleated osteoclasts on eroded surfaces per millimeter of cancellous perimeter. All histomorphometric measurements were performed with the Osteomeasure Analysis system (Osteometrics, Atlanta, GA).

Micro-CT (μCT) scans of lumbar vertebrae and femurs

The left femurs and lumbar spines were placed in 70% ethanol and were scanned at a resolution of 8 μm using an in-house μCT system (Physiological Imaging Research Laboratory, Mayo Clinic, Rochester, MN) in all three dimensions as described by Jorgensen *et al.* (26).

Serum testosterone (T), estradiol (E_2), and IGF-I measurements

Serum T and E_2 were measured by RIA kits (Diagnostic Systems Laboratories Inc., Webster, TX, for T, and Diagnostic Products Corp., Los Angeles, CA, for E_2 , respectively). The interassay variability was less than 7% and less than 10% for T and E_2 , respectively. Serum IGF-I measurements were made using an IGF-I (IGF binding protein blocked) RIA kit (American Laboratory Products, Windham, NH). The interassay CV was less than 6%.

Statistical tests

All data are presented as mean \pm SEM, except for serum T where the median values and the interquartile range are reported (due to the skewness of the data). Comparisons between specific genotypes were done using two-tailed t tests, and $P < 0.05$ was considered significant.

Results

Body weights and bone lengths

Body weights and femur lengths were identical in the $ER\alpha^{+/+}$ and $ER\alpha^{+/-}$ mice. However, these parameters were reduced in both the $ER\alpha^{+/NERKI}$ and $ER\alpha^{-/NERKI}$ mice, compared with the $ER\alpha^{+/+}$ controls (Fig. 1). These differences largely persisted until 25 wk of age, with the exception that body weights in the $ER\alpha^{-/NERKI}$ mice, although lower than in the $ER\alpha^{+/+}$ mice, were not statistically different at the later time points. The femur lengths of the $ER\alpha^{+/NERKI}$ mice were significantly lower than the $ER\alpha^{+/-}$ mice at least up to 20 wk.

Impact of the *NERKI* allele on axial and appendicular bone in male mice

Total aBMD at the lumbar spine (L1-L4) and femur by DXA and the total vBMD at the proximal tibial metaphysis

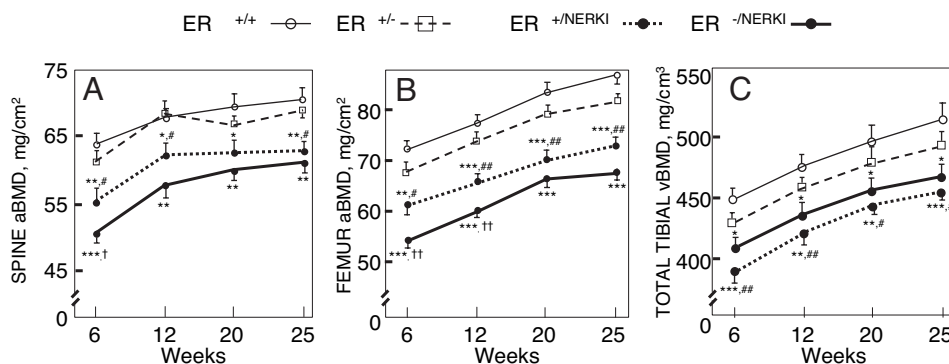


FIG. 2. Total aBMD measurements using DXA scans of the lumbar spine (A), femur (B), and total vBMD (C) scans using pQCT of the proximal tibial metaphysis ($n = 10/\text{genotype}$ per time point). *, $P < 0.05$, **, $P < 0.01$, ***, $P < 0.001$ vs. $ER\alpha^{+/+}$ mice; #, $P < 0.05$, ##, $P < 0.01$ vs. $ER\alpha^{+/-}$ mice; †, $P < 0.05$, ††, $P < 0.01$ vs. $ER\alpha^{+/NERKI}$ mice.

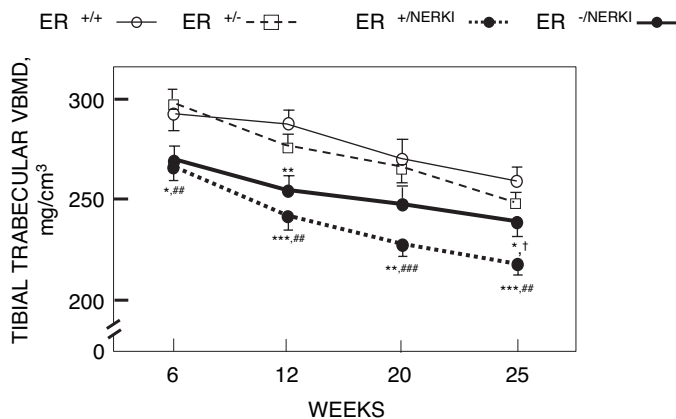


FIG. 3. Trabecular vBMD measurements using pQCT at the proximal tibial metaphysis (n = 10/genotype per time point). *, P < 0.05, **, P < 0.01, ***, P < 0.001 vs. ER $\alpha^{+/+}$ mice; ##, P < 0.01, ###, P < 0.001 vs. ER $\alpha^{+/-}$ mice; †, P < 0.05 vs. ER $\alpha^{+/NERKI}$ mice.

by pQCT were significantly reduced at all time points in both the ER $\alpha^{+/NERKI}$ and ER $\alpha^{-/NERKI}$ mice, compared with ER $\alpha^{+/+}$ mice (Fig. 2, A–C). Additionally, the reduction in these parameters was more severe in the ER $\alpha^{+/NERKI}$, compared with ER $\alpha^{+/-}$ mice. As is also evident, the deficits in BMD at these sites (at least for aBMD at the spine and femur) tended to be more severe in the ER $\alpha^{-/NERKI}$, compared with the ER $\alpha^{+/NERKI}$ mice.

Deficits in bone parameters are not compartment specific in male mice harboring the NERKI allele

To evaluate whether the osteopenia was localized to either the trabecular or cortical bone compartments, we measured trabecular vBMD at the tibial metaphysis and cortical vBMD at the tibial metaphysis and diaphysis using pQCT. Trabecular vBMD in both the ER $\alpha^{+/NERKI}$ and ER $\alpha^{-/NERKI}$ male mice were reduced, compared with their ER $\alpha^{+/+}$ wild-type littermates. The ER $\alpha^{+/NERKI}$ mice also displayed a significant reduction, compared with ER $\alpha^{+/-}$ mice (Fig. 3). Interestingly, at wk 25, the reduction in trabecular vBMD in the heterozygote (ER $\alpha^{+/NERKI}$) mice was even more severe than in mice lacking an intact ER α allele (ER $\alpha^{-/NERKI}$) (P < 0.05).

Cortical vBMD and thickness were significantly but equally reduced in both the ER $\alpha^{+/NERKI}$ and ER $\alpha^{-/NERKI}$, compared with ER $\alpha^{+/+}$ mice at the metaphysis (Fig. 4, A and B). A significant reduction in these parameters was also observed at the tibial diaphysis, a more robust site for cortical bone (Fig. 4, C and D). However, at this site, the reductions in cortical vBMD and thickness were more severe in the ER $\alpha^{-/NERKI}$ mice, compared with ER $\alpha^{+/NERKI}$ mice at most of the time points. The ER $\alpha^{+/NERKI}$ mice also displayed a significant reduction, compared with ER $\alpha^{+/-}$ mice, in all the above cortical parameters at both the metaphyseal and diaphyseal sites at most of the time points studied.

Trabecular structure is affected differently in ER $\alpha^{+/NERKI}$ vs. ER $\alpha^{-/NERKI}$ male mice

Histomorphometric evaluation of trabecular bone parameters at the lumbar spine revealed some similarities but also important differences between ER $\alpha^{+/NERKI}$ and ER $\alpha^{-/NERKI}$ mice. In agreement with the aBMD data at the spine (Fig. 2A) and the trabecular vBMD at the tibial metaphysis (Fig. 3), both the ER $\alpha^{+/NERKI}$ and ER $\alpha^{-/NERKI}$ mice had reduced bone volumes (BVs)/tissue volume (TVs), compared with ER $\alpha^{+/+}$ mice (Table 1). However, the structural basis for the reductions in BV/TVs in the ER $\alpha^{+/NERKI}$ vs. the ER $\alpha^{-/NERKI}$ mice was quite different. Thus, the predominant defect in the ER $\alpha^{+/NERKI}$ mice was a reduction in trabecular number (TbN) with increased trabecular separation, whereas the ER $\alpha^{-/NERKI}$ mice had preserved TbN but greater reductions in trabecular thickness. To further understand the cellular basis for this, we calculated the osteoblast numbers per bone perimeter, MAR and BFR as markers of osteoblastic activity, and osteoclast numbers and percent eroded surface/bone surface as indices of osteoclastic activity at this site. Compared with ER $\alpha^{+/+}$ mice, osteoblast numbers, MAR, and BFR were significantly reduced in the ER $\alpha^{-/NERKI}$ but not ER $\alpha^{+/NERKI}$ mice. By contrast, the osteoclast numbers and eroded surface/bone surface was significantly elevated in the ER $\alpha^{+/NERKI}$ but not ER $\alpha^{-/NERKI}$ mice. The ER $\alpha^{+/NERKI}$ mice did, however, display a trend toward a decrease in osteoblast numbers as well (P = 0.059).

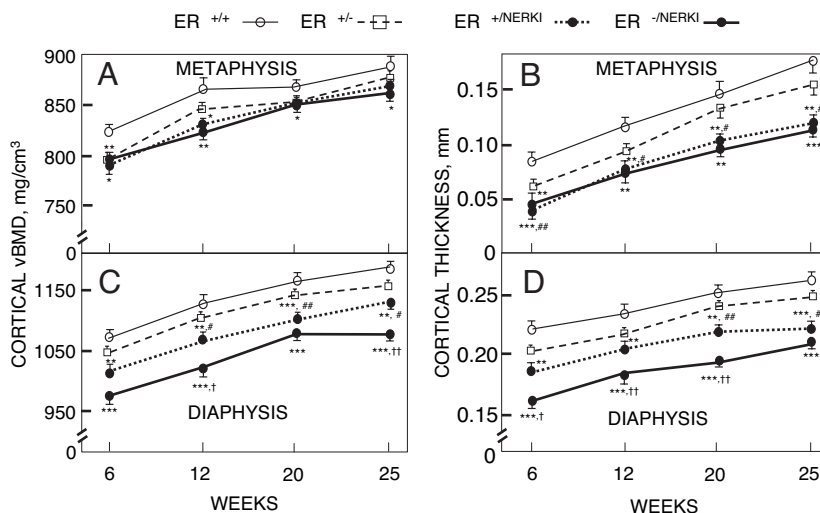


FIG. 4. Cortical vBMDs at the metaphysis (A) and diaphysis (C) and cortical thicknesses at the metaphysis (B) and diaphysis (D) of the tibia as measured by pQCT scans (n = 10/genotype per time point). *, P < 0.05, **, P < 0.01, ***, P < 0.001 vs. ER $\alpha^{+/+}$ mice; #, P < 0.05, ##, P < 0.01 vs. ER $\alpha^{+/-}$ mice; †, P < 0.05, ††, P < 0.01 vs. ER $\alpha^{+/NERKI}$ mice.

TABLE 1. Static and dynamic histomorphometric parameters for trabecular bone at the lumbar vertebrae in ER $\alpha^{+/+}$, ER $\alpha^{+/-}$, and ER $\alpha^{-/-}$ male mice (n = 5–10/genotype)

Histomorphometric parameters	ER $\alpha^{+/+}$	ER $\alpha^{+/-}$	ER $\alpha^{-/-}$
BV/TV (%)	26.6 ± 2.5	17.4 ± 1.1**	18.4 ± 1.4**
Trabecular number (per millimeter)	4.75 ± 0.3	3.82 ± 0.02*	4.71 ± 0.24††
Trabecular thickness (μm)	55.6 ± 2.5	45.5 ± 2.0**	38.9 ± 2.0***,†
Trabecular separation (μm)	159.7 ± 14.5	220.8 ± 14.6**	176.3 ± 11.8†
MAR (μm/d)	0.42 ± 0.03	0.41 ± 0.03	0.22 ± 0.02***,††
BFR/BV (%/d)	0.12 ± 0.03	0.17 ± 0.04	0.02 ± 0.004***,††
Eroded surface/bone surface (%)	1.89 ± 0.34	10.8 ± 1.8**	1.84 ± 0.5††
Osteoblast no./bone perimeter (per millimeter)	8.65 ± 1.04	5.23 ± 1.05 ^a	2.53 ± 0.43***, ^b
Osteoclast no./bone perimeter (per millimeter)	2.00 ± 0.47	5.82 ± 0.95*	1.54 ± 0.4††

* $P < 0.05$, ** $P < 0.01$, *** $P < 0.001$, ^a $P = 0.059$ vs. ER $\alpha^{+/+}$ mice.
 † $P < 0.05$, †† $P < 0.01$, ^b $P = 0.062$ vs. ER $\alpha^{+/-}$ mice.

Effect of the NERKI allele on radial bone growth in male mice

Both the ER $\alpha^{+/-}$ and ER $\alpha^{-/-}$ mice had significantly reduced cortical periosteal circumferences at the metaphysis (Fig. 5A) and diaphysis (Fig. 5C). The reduction in the periosteal circumference was significantly greater in the ER $\alpha^{-/-}$ mice, compared with the ER $\alpha^{+/-}$ mice, at all time points ($P < 0.05$), and at least at the diaphysis, periosteal circumference was also lower in the ER $\alpha^{+/-}$, compared with the ER $\alpha^{+/+}$ mice. Endosteal circumference was also significantly reduced in the ER $\alpha^{-/-}$, compared with the ER $\alpha^{+/+}$ mice, with the ER $\alpha^{+/-}$ mice having intermediate values (Fig. 5, B and D). These changes in periosteal and endosteal dimensions were accompanied by a significant reduction in periosteal MAR in the ER $\alpha^{-/-}$, compared with the ER $\alpha^{+/+}$ mice (Fig. 6A); however, we could not detect any statistically significant difference in endosteal MAR between the two genotypes (Fig. 6B).

Alterations in bone strength indices

Because the metaphyseal bone site primarily experiences compressive loading, we calculated the CSI as indicative of the ability of the tibia in the ER $\alpha^{+/-}$, ER $\alpha^{+/-}$, and ER $\alpha^{-/-}$ to resist compressive loads and compared it to wild-type ER $\alpha^{+/+}$ mice. Both the ER $\alpha^{+/-}$ and ER $\alpha^{-/-}$

mice displayed significant reductions in their ability to tolerate compressive loads at the tibial metaphysis, compared with ER $\alpha^{+/+}$ mice at both the initial (6 wk) and final (25 wk) time points ($P < 0.05$) (Table 2). The cortical BSI, which is a high-fidelity predictor of cortical bone-bending strength, was calculated for the tibial diaphysis. Both the ER $\alpha^{+/-}$ and ER $\alpha^{-/-}$ mice had significantly reduced BSI at the initial 6- and final 25-wk time point ($P < 0.01$ vs. ER $\alpha^{+/+}$). Interestingly, the reduction in bone strength was more severe in ER $\alpha^{-/-}$ mice, compared with ER $\alpha^{+/-}$ mice ($P < 0.01$). To assess the ability of the cortical bone to resist torsional deformation, the cortical cross-sectional moment of inertia and cortical moment of resistance were calculated for the tibial metaphysis and diaphysis in all the mice in the study. At both these sites, the ER $\alpha^{+/-}$ and ER $\alpha^{-/-}$ mice exhibited significant reductions, compared with wild-type littermates in these parameters ($P < 0.01$ and $P < 0.001$ vs. ER $\alpha^{+/+}$, respectively). The reductions in the above parameters were also more severe in the ER $\alpha^{+/-}$ heterozygotes, compared with ER $\alpha^{+/-}$ heterozygotes. At the diaphysis, however, the reduction in torsional strength was significantly more in ER $\alpha^{-/-}$ mice vs. ER $\alpha^{+/-}$ mice ($P < 0.01$). It should be noted that an exactly similar pattern was observed in all the above parameters at the intermediate

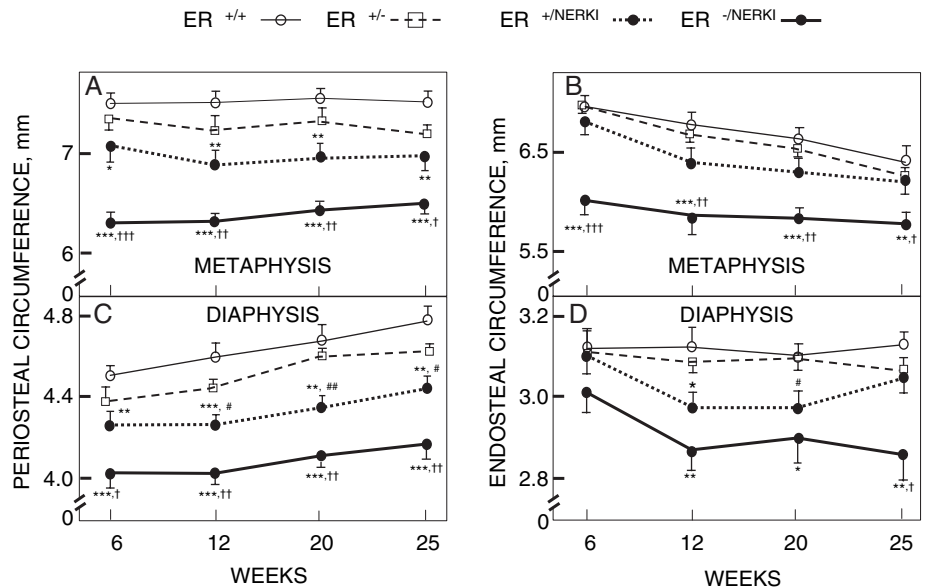


FIG. 5. Periosteal circumferences at the metaphysis (A) and diaphysis (C) and endosteal circumferences at the metaphysis (B) and diaphysis (D) of the tibia derived from pQCT scans (n = 10/genotype per time point). * $P < 0.05$, ** $P < 0.01$, *** $P < 0.001$ vs. ER $\alpha^{+/+}$ mice; # $P < 0.05$, ## $P < 0.01$ vs. ER $\alpha^{+/-}$ mice; † $P < 0.05$, †† $P < 0.01$, ††† $P < 0.001$ vs. ER $\alpha^{+/-}$ mice.

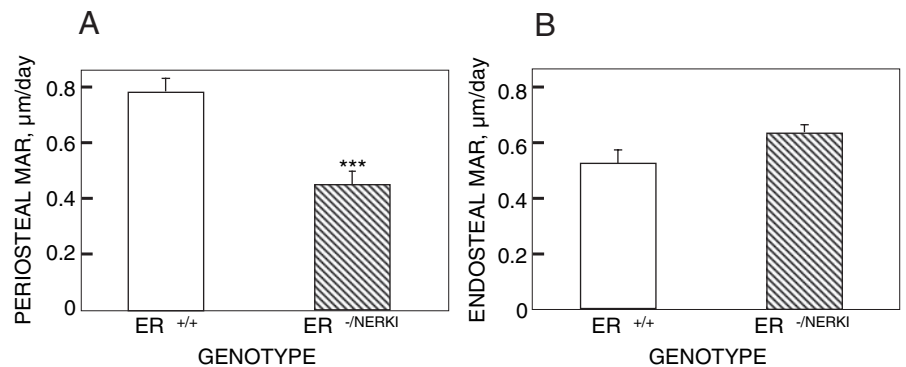


FIG. 6. MAR at the periosteal (A) and endosteal (B) surfaces of the femur diaphysis in $ER\alpha^{+/+}$ and $ER\alpha^{-/NERKI}$ mice calculated histomorphometrically ($n = 10/\text{genotype}$). ***, $P < 0.001$ vs. $ER\alpha^{+/+}$ mice.

time points (12 and 20 wk, data not shown) and that these biomechanical indices likely reflect in large part the smaller bones in the $ER\alpha^{+/NERKI}$ and $ER\alpha^{-/NERKI}$ mice. From Table 2, it is also evident that the $ER\alpha^{+/-}$ mice displayed reductions in at least some biomechanical parameters with respect to $ER\alpha^{+/+}$ mice. However, the $ER\alpha^{+/NERKI}$ heterozygotes displayed reductions in BSIs to an extent much greater than the $ER\alpha^{+/-}$ heterozygous mice for most of the parameters at the time points analyzed.

μ CT analysis

Figure 7 provides a visual demonstration, using μ CT, of the bone phenotype of the $ER\alpha^{-/NERKI}$ vs. the $ER\alpha^{+/+}$ mice. As is evident, $ER\alpha^{-/NERKI}$ mice had thinner cortices and smaller diameters at the femur metaphysis and diaphysis and significantly reduced trabecular bone at both the metaphysis and lumbar spine.

Serum sex steroid and IGF-I levels in $ER\alpha^{-/NERKI}$ male mice

Table 3 shows serum levels of E_2 , T, and IGF-I in the $ER\alpha^{+/+}$ and $ER\alpha^{-/NERKI}$ mice. Serum E_2 levels were virtually identical in the two groups. Whereas the median serum T levels were higher in the $ER\alpha^{-/NERKI}$, compared with the $ER\alpha^{+/+}$ mice, these differences were not statistically significant due to the wide variability of T levels in the $ER\alpha^{+/+}$ mice. Serum IGF-I levels were, however, clearly reduced in the $ER\alpha^{-/NERKI}$, compared with the $ER\alpha^{+/+}$ mice.

Discussion

This study describes the consequences of the alteration of the balance between the classical and nonclassical $ER\alpha$ signaling pathways on the skeleton of male mice. Our results indicate that either the attenuation (as in the $ER\alpha^{+/NERKI}$ mice) or complete loss (as in the $ER\alpha^{-/NERKI}$ mice) of classical $ER\alpha$ signaling profoundly impacts the male murine skeleton. Both the $ER\alpha^{+/NERKI}$ and $ER\alpha^{-/NERKI}$ males have reduced femur lengths and osteopenia in the axial (vertebrae) and appendicular (femur, tibia) skeleton, compared with $ER\alpha^{+/+}$ or $ER\alpha^{+/-}$ littermates at almost all ages. These mutant mice also display deficits in trabecular and cortical bone. The reductions in cortical bone parameters were generally more severe in the $ER\alpha^{-/NERKI}$ mice, compared with their heterozygote $ER\alpha^{+/NERKI}$ littermates. This was similar to the observed effect of the $NERKI$ allele in female mice, in which the

severity of cortical osteopenia was allele dose dependent, with mice totally devoid of classical $ER\alpha$ signaling ($ER\alpha^{-/NERKI}$ female mice) exhibiting a greater reduction in all cortical bone parameters, compared with $ER\alpha^{+/NERKI}$ heterozygote females (24). That there indeed exists an allele dose dependency is further strengthened by the observation that the skeletal deficits in the $ER\alpha^{+/NERKI}$ heterozygote males were significant, compared with their wild-type heterozygous $ER\alpha^{+/-}$ littermates at most of the time points scanned, consistent with effects of the $NERKI$ receptor beyond just those of loss one allele of the receptor.

However, in contrast to female $ER\alpha^{+/NERKI}$ and $ER\alpha^{-/NERKI}$ mice, in which trabecular bone was preserved at different sites, their male counterparts displayed significant reductions in BMD and BV/TV at the same sites (the lumbar vertebrae and the proximal tibial metaphysis). Previously our group (25) and others (27, 28) demonstrated that cortical bone predominantly contains $ER\alpha$ with little or no $ER\beta$, whereas trabecular bone contains both receptors, with $ER\beta$ perhaps more abundantly expressed. The fact that male $ER\alpha^{+/NERKI}$ and $ER\alpha^{-/NERKI}$ mice displayed reduced trabecular BMD and BV/TV whereas their female counterparts did not can perhaps be explained by these findings combined with data from previous studies of male $ER\alpha$ knockout mice (8, 9). Thus, using $ER\alpha^{-/-}$ male mice, Vidal *et al.* (8) demonstrated that $ER\alpha$, but not $ER\beta$, mediated the important effects of E on the murine male skeleton during growth and development. This was independently confirmed by Sims *et al.* (9) using $ER\alpha^{-/-}$ males generated by another group (11). Furthermore, in contrast to ovx female $ER\alpha^{-/-}$ mice who were partially responsive to E, orchietomized or intact male $ER\alpha^{-/-}$ mice did not show any response to E in trabecular bone (10, 29), suggesting that whereas $ER\beta$ was able to mediate effects of E on bone in female mice, it was unable to do so in male mice. It is therefore possible that the attenuation or loss of classical signaling by $ER\alpha$ in male trabecular bone in the absence of compensatory $ER\beta$ action [as appears to be present in female mice (9)] results in the observed deficits in trabecular bone in male $ER\alpha^{+/NERKI}$ and $ER\alpha^{-/NERKI}$ mice, compared with preserved trabecular bone parameters in female $ER\alpha^{+/NERKI}$ and $ER\alpha^{-/NERKI}$ mice. Similar sexual dimorphisms in bone parameters has been observed before in other generically altered mouse models, *i.e.* aromatase knockout mice (4, 5). Thus, Oz *et al.* (4) found that the femur length was decreased in male, but not female, aromatase knockout mice, and changes in bone remodeling were quite

TABLE 2. Biomechanical parameters obtained by pQCT at the tibial metaphysis and diaphysis in ER $\alpha^{+/+}$, ER $\alpha^{+/-}$, ER $\alpha^{+/NERKI}$, and ER $\alpha^{-/NERKI}$ male mice (n = 9–10/genotype)

Biomechanical parameters	Wk 6				Wk 25			
	ER $\alpha^{+/+}$	ER $\alpha^{+/-}$	ER $\alpha^{+/NERKI}$	ER $\alpha^{-/NERKI}$	ER $\alpha^{+/+}$	ER $\alpha^{+/-}$	ER $\alpha^{+/NERKI}$	ER $\alpha^{-/NERKI}$
Tibial metaphysis								
CSI	94.6 ± 2.8	88.8 ± 2.8	77.6 ± 2.2***##	72.5 ± 1.9*	109 ± 3.4	99.9 ± 2.2	89.2 ± 2***##	85.4 ± 1.8*
Cortical cross-sectional moment of inertia (mm ⁴)	0.56 ± 0.05	0.39 ± 0.04*	0.24 ± 0.04***##	0.19 ± 0.02***	1.22 ± 0.08	0.95 ± 0.06*	0.68 ± 0.07***#	0.52 ± 0.02***
Cortical moment of resistance (mm ⁵)	0.41 ± 0.03	0.30 ± 0.03*	0.18 ± 0.02***##	0.16 ± 0.01***	0.85 ± 0.06	0.65 ± 0.04*	0.47 ± 0.05***#	0.38 ± 0.03***
Tibial diaphysis								
BSI	236.9 ± 14.5	203 ± 13.0	169.3 ± 16**	118.4 ± 7.7**†	384.4 ± 27.4	327 ± 14	250.2 ± 17***	183 ± 10.8***††
Cortical cross-sectional moment of inertia (mm ⁴)	0.22 ± 0.01	0.19 ± 0.01	0.17 ± 0.01**	0.12 ± 0.007***†	0.32 ± 0.02	0.28 ± 0.01	0.22 ± 0.01***##	0.17 ± 0.009***††
Cortical moment of resistance (mm ⁵)	0.29 ± 0.01	0.26 ± 0.01*	0.23 ± 0.01**	0.17 ± 0.007***††	0.37 ± 0.01	0.34 ± 0.01*	0.28 ± 0.01***##	0.23 ± 0.008***††

* $P < 0.05$, ** $P < 0.01$, *** $P < 0.001$ vs. ER $\alpha^{+/+}$ mice.

$P < 0.05$, ## $P < 0.01$ vs. ER $\alpha^{+/-}$ mice.

† $P < 0.05$, †† $P < 0.01$ vs. ER $\alpha^{+/NERKI}$ mice.

different in male *vs.* female aromatase knockout mice. Miyaura *et al.* (5) also reported that the degree of bone loss in 32-wk-old aromatase knockout mice was more severe in females than males. Finally, because we do not have data on serum testosterone levels in the ER $\alpha^{+/NERKI}$ mice, it is possible that alterations in sex steroid levels in these mice could be contributing to the skeletal phenotype and differences from the phenotype observed in the corresponding female mice.

The trabecular and cortical bone phenotype in the male ER $\alpha^{+/NERKI}$ and ER $\alpha^{-/NERKI}$ mice was present from the earliest time point studied (6 wk), suggesting that the skeletal changes we observed were developmental. However, the importance of the role of classical ER α signaling in murine bone maintenance was previously demonstrated by our studies using ovx female ER $\alpha^{-/NERKI}$ mice, who have an attenuated response to estrogen in trabecular bone and an aberrant response to estrogen in cortical bone, whereas ER $\alpha^{+/NERKI}$ female mice display attenuated responses to estrogen in both trabecular and cortical bone (24). Nonetheless, we recognize that analogous studies need to be done in the male mice to establish a role for classical ER signaling in the maintenance of bone in male ER $\alpha^{-/NERKI}$ mice.

Although the trabecular BV/TVs in the ER $\alpha^{+/NERKI}$ and ER $\alpha^{-/NERKI}$ male mice were significantly reduced, compared with their wild-type littermates, the structural basis for this reduction appeared to differ in the ER $\alpha^{+/NERKI}$ *vs.* the ER $\alpha^{-/NERKI}$ mice. ER $\alpha^{+/NERKI}$ mice predominantly had a decrease in TbN and increase in TbSp due to an increase in osteoclastic activity, as evidenced by a significant increase in osteoclast numbers and trabecular eroded surfaces, with no change in BFRs, although there was a trend for reduced osteoblast numbers. By contrast, the major defect in the ER $\alpha^{-/NERKI}$ mice was a decrease in TbTh, resulting from a decrease in osteoblastic activity due to significant decreases in osteoblast numbers and MAR and BFR. These abnormal patterns of osteoclastic and osteoblastic activities in the ER $\alpha^{+/NERKI}$ *vs.* the ER $\alpha^{-/NERKI}$ mice suggest that bone formation and resorption are affected in distinct ways after either attenuation or loss of classical ER α signaling in trabecular bone in male mice, respectively.

The retardation in cortical radial bone growth was more severe in the ER $\alpha^{-/NERKI}$ mice at the periosteal surface, compared with ER $\alpha^{+/+}$ and ER $\alpha^{+/NERKI}$ mice, although the latter also displayed significant reductions in periosteal circumference, compared with wild-type mice. At the endosteal surface of cortical bone, the complete loss of classical ER α signaling (ER $\alpha^{-/NERKI}$ mice) did not seem to lead to enhanced expansion, as was previously seen with female ER $\alpha^{-/NERKI}$ mice (24). That this observed radial growth pattern was associated with decreased osteoblastic activity at the periosteal (but not endosteal) surface was confirmed by measuring the MARs at these surfaces. Thus, it appears that the difference in osteoblastic activity at these two surfaces accounts for the observed phenotype.

IGF-I regulates peak bone density in mice during prepuberty predominantly via GH-independent mechanisms and during puberty via both GH-independent and -dependent mechanisms (30), and a lack of IGF-I has been shown to exaggerate effects of calcium deficiency on murine bone accretion (31). However, the exact contribution of circulating *vs.* locally produced IGF-I on bone parameters is still unclear

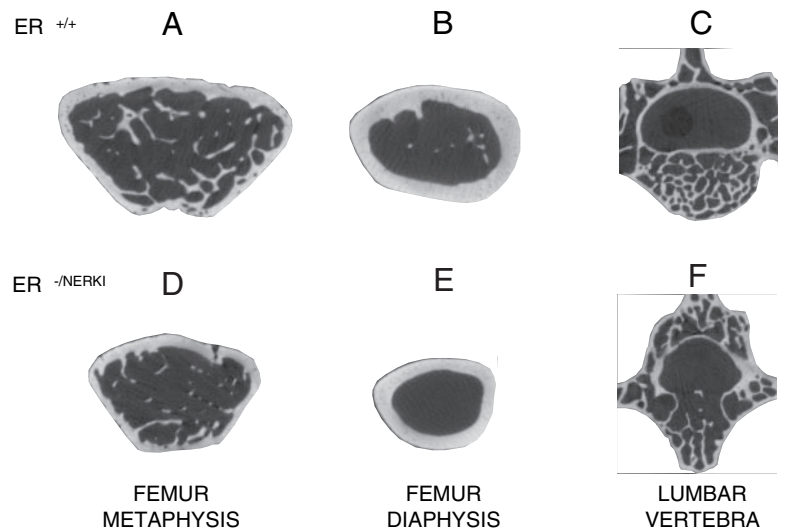


FIG. 7. μ CT images at an 8- μ m resolution of the femur and lumbar vertebrae in $ER\alpha^{+/+}$ and $ER\alpha^{-/NERKI}$ male mice. Representative cross-sections of proximal femur metaphysis (A), femur diaphysis (B), and lumbar vertebra (C) of $ER\alpha^{+/+}$ male mice, and proximal femur metaphysis (D), femur diaphysis (E), and lumbar vertebra (F) of $ER\alpha^{-/NERKI}$ male mice. The marked reduction in trabecular and cortical bone in $ER\alpha^{-/NERKI}$, compared with $ER\alpha^{+/+}$, male mice is evident.

(32, 33). For example, in liver IGF-I knockout mice, longitudinal bone growth was not impaired (34). This has led to the suggestion that only the IGF-I produced locally by bone cells is important for linear growth (33). A subsequent study using mice knocked out for liver IGF-I (LIDKO) and labile subunit (ALSKO) and both (LID-ALSKO) concluded that a threshold serum IGF-I concentration greater than what was observed in the LID-ALSKO mice (85.2 ng/ml) was necessary for linear and appositional bone growth (30). In this context, serum IGF-I levels in $ER\alpha^{-/NERKI}$ male mice were significantly reduced, compared with the $ER\alpha^{+/+}$ mice, which could explain the shorter bones and reduced periosteal expansion in the $ER\alpha^{-/NERKI}$ mice. Of note, however, we observed a similar reduction in IGF-I levels in our previous study with $ER\alpha^{-/NERKI}$ female mice (24), but trabecular bone parameters were preserved in these mice. In the present study, the levels of serum IGF-I observed in the $ER\alpha^{-/NERKI}$ male mice (156.1 ng/ml) are comparable with LID-ALSKO control mice (151.4 ng/ml) and 3-fold greater than those observed in the LID-ALSKO mice (55.19 ng/ml) described in the study by Yakar *et al.* (32). Thus, although the reduction in serum IGF-I levels could be a contributive factor, it cannot completely explain the reduction in radial and longitudinal bone parameters in the $ER\alpha^{-/NERKI}$ male mice observed in the present study, and it is likely that the NERKI receptor has independent effects on bone growth and/or mass that require further study.

Because the present study describes the consequences of either partial ($ER\alpha^{+/NERKI}$) or complete ($ER\alpha^{-/NERKI}$) loss of classical $ER\alpha$ signaling on the male skeleton, it is important to place the findings of the present study in the context of

previous studies by others in male $ER\alpha$ knockout mice ($ER\alpha^{-/-}$ mice) (8, 9, 35) to arrive at a better understanding of the importance of the classical and nonclassical estrogen signaling pathways in male bone. Indeed, earlier studies with $ER\alpha^{-/-}$ mice have provided important insights into estrogen action in male bone through this receptor, although the mice used in two of these studies (8, 35), expressed a splice variant of $ER\alpha$. Sims *et al.* (9), using male $ER\alpha^{-/-}$ mice, which did not express a splice variant, showed that complete deletion of $ER\alpha$ led to decreases in bone size, bone turnover, cortical thickness, and density and periosteal MAR and parallel increases in serum T and trabecular BV. Vidal *et al.* (8) and Parikka *et al.* (35) studied young (0.5–4 months) and old (1 yr) male $ER\alpha^{-/-}$ mice, respectively, in whom a splice variant of the $ER\alpha$ was expressed. Their studies collectively described decreases in serum IGF-I levels, bone size, cortical thickness and area, periosteal and endosteal circumferences, and reductions in the biomechanical strength of cortical bone as assessed by a decrease in the cross-sectional moment of inertia at the femur diaphysis. An increase in trabecular density and volume was also observed in these mice at 1 yr with a parallel increase in serum T levels (35). Thus, similar to $ER\alpha^{-/-}$ males described in the above studies, the $ER\alpha^{-/NERKI}$ males described in the present study display significant reductions in bone size, cortical bone densitometric and biomechanical parameters, and serum IGF-I levels. Whereas serum E_2 levels were normal in the $ER\alpha^{-/NERKI}$ and $ER\alpha^{-/-}$ males and serum T levels were not statistically different in $ER\alpha^{-/NERKI}$, compared with their wild-type littermates, $ER\alpha^{-/-}$ males had markedly elevated levels of serum T (4-fold). The increased T levels in the $ER\alpha^{-/-}$ males likely

TABLE 3. Serum sex steroid and IGF-I levels in the $ER\alpha^{+/+}$ and $ER\alpha^{-/NERKI}$ male mice (n = 10/genotype)

Serum measurements	$ER\alpha^{+/+}$	$ER\alpha^{-/NERKI}$
E_2 (pmol/liter)	15.3 \pm 3.1	17.1 \pm 3.1
T (nmol/liter) ^a	2.71 (0.9–58.6)	7.8 (3.1–15.3)
IGF-I (ng/ml)	289.4 \pm 10.05	156.1 \pm 7.54 ^{***}

E_2 and T measurements were done at 3 months of age, and serum IGF-I measurements were done at the end of the study at approximately 6 months of age.

^a Values are reported as median (interquartile range 25th to 75th percentile).

*** $P < 0.001$ vs. $ER\alpha^{+/+}$ mice.

explain the increase in trabecular vBMD and BV/TV present in these mice. Our data also demonstrate that loss of classical ERE signaling results in significant reductions in trabecular vBMD and BV/TV, associated with trabecular thinning. Collectively, however, the overall similarity in the skeletal phenotype of the ER $\alpha^{-/-}$ and ER $\alpha^{-/NERKI}$ mice (with the added deficits in trabecular bone in the ER $\alpha^{-/NERKI}$ mice) clearly demonstrates the importance not only of ER α but rather also of classical ERE signaling pathways for male bone in mice and that shifting the balance solely toward the nonclassical pathway can have suppressive effects on bone gain.

Acknowledgments

We thank Donna Jewison for performing the sectioning of the mouse bones, Kelly Hoey for technical assistance, and James Peterson for help with statistical analyses and preparation of the figures.

Received August 28, 2006. Accepted December 21, 2006.

Address all correspondence and requests for reprints to: Sundeeep Khosla, M.D., 5-194 Joseph, Endocrine Research Unit, Mayo Clinic College of Medicine, 200 First Street SW, Rochester, Minnesota 55905. E-mail: khosla.sundeeep@mayo.edu.

This work was supported by National Institutes of Health Grants P01 AG004875 (to T.C.S. and S.K.) and P01 HD21921 (to J.L.J.).

Disclosure Statement: The authors have nothing to disclose.

References

- Smith EP, Boyd J, Frank GR, Takahashi H, Cohen RM, Specker B, Williams TC, Lubahn DB, Korach KS 1994 Estrogen resistance caused by a mutation in the estrogen-receptor gene in a man. *N Engl J Med* 331:1056–1061
- Carani C, Qin K, Simoni M, Faustini-Fustini M, Serpente S, Boyd J, Korach KS, Simpson ER 1997 Effect of testosterone and estradiol in a man with aromatase deficiency. *N Engl J Med* 337:91–95
- Bilezikian JP, Morishima A, Bell J, Grumbach MM 1998 Increased bone mass as a result of estrogen therapy in a man with aromatase deficiency. *N Engl J Med* 339:599–603
- Oz OK, Zerwekh JE, Fisher C, Graves K, Nanu L, Millsaps R, Simpson ER 2000 Bone has a sexually dimorphic response to aromatase deficiency. *J Bone Miner Res* 15:507–514
- Miyaura C, Toda K, Inada M, Ohshiba T, Matsumoto C, Okada T, Ito M, Shizuta Y, Ito A 2001 Sex- and age-related response to aromatase deficiency in bone. *Biochem Biophys Res Commun* 280:1062–1068
- Peng Z-Q, Li X-D, Makela S, Vaananen HK, Poutanen M 2004 Skeletal changes in transgenic male mice expressing human cytochrome P450 aromatase. *J Bone Miner Res* 19:1320–1328
- Spelsberg TC, Subramaniam M, Riggs BL, Khosla S 1999 The actions and interactions of sex steroids and growth factors/cytokines on the skeleton. *Mol Endocrinol* 13:819–828
- Vidal O, Lindberg MK, Hollberg K, Baylink DJ, Andersson G, Lubahn DB, Mohan S, Gustafsson J, Ohlsson C 2000 Estrogen receptor specificity in the regulation of skeletal growth and maturation in male mice. *Proc Natl Acad Sci USA* 97:5474–5479
- Sims NA, Dupont S, Krust A, Clement-LaCroix P, Minet D, Resche-Rigon M, Gaillard-Kelly M, Baron R 2002 Deletion of estrogen receptors reveals a regulatory role for estrogen receptors β in bone remodeling in females but not in males. *Bone* 30:18–25
- Sims NA, Clement-LaCroix P, Minet D, Fraslon-Vanhulle C, Gaillard-Kelly M, Resche-Rigon M, Baron R 2003 A functional androgen receptor is not sufficient to allow estradiol to protect bone after gonadectomy in estradiol receptor-deficient mice. *J Clin Invest* 111:1319–1327
- Dupont S, Krust A, Gansmuller A, Dierich A, Chambon P, Mark M 2000 Effect of single and compound knockouts of estrogen receptors α (ER α) and β (ER β) on mouse reproductive phenotypes. *Development* 127:4277–4291
- Beato M, Herrlich P, Schutz G 1995 Steroid hormone receptors: many actors in search of a plot. *Cell* 83:851–857
- Maurer RA, Notides AC 1987 Identification of an estrogen-responsive element from the 5'-flanking region of the rat prolactin gene. *Mol Cell Biol* 7:4247–4254
- Savouret J-F, Bailly A, Misrahi M, Rauch C, Redeuilh G, Chachereau A, Milgrom E 1991 Characterization of the hormone responsive element involved in the regulation of the progesterone receptor gene. *EMBO J* 10:1875–1883
- Weisz A, Rosales R 1990 Identification of an estrogen response element upstream of the human *c-fos* gene that binds the estrogen receptor and the AP-1 transcription factor. *Nucleic Acids Res* 18:5097–5106
- Paech K, Webb P, Kuiper GGJM, Nilsson S, Gustafsson JA, Kushner PJ, Scanlan TS 1997 Differential ligand activation of estrogen receptors ER α and ER β at AP1 sites. *Science* 277:1508–1510
- Umayahara Y, Kawamori R, Watada H, Imano E, Iwama N, Morishima T, Yamasaki Y, Kajimoto Y, Kamada T 1994 Estrogen regulation of the insulin-like growth factor I gene transcription involves an AP-1 enhancer. *J Biol Chem* 269:16433–16441
- Ray A, Prefontaine KE, Ray P 1994 Down-modulation of interleukin-6 gene expression by 17 β -estradiol in the absence of high affinity DNA binding by the estrogen receptor. *J Biol Chem* 269:12940–12946
- Levin ER 2005 Integration of the extranuclear and nuclear actions of estrogen. *Mol Endocrinol* 19:1951–1959
- Manolagas SC, Kousteni S 2001 Perspective: nonreproductive sites of action of reproductive hormones. *Endocrinology* 142:2200–2204
- Cheung E, Acevedo ML, Cole PA, Kraus WL 2005 Altered pharmacology and distinct coactivator usage for estrogen receptor-dependent transcription through activating protein-1. *Proc Natl Acad Sci USA* 102:559–564
- Jakacka M, Ito M, Martinson F, Ishikawa T, Lee EJ, Jameson JL 2002 An estrogen receptor (ER) α deoxyribonucleic acid-binding domain knock-in mutation provides evidence for nonclassical ER pathway signaling *in vivo*. *Mol Endocrinol* 16:2188–2201
- Jakacka M, Ito M, Weiss J, Chien P-Y, Gehm BD, Jameson JL 2001 Estrogen receptor binding to DNA is not required for its activity through the nonclassical AP1 pathway. *J Biol Chem* 276:13615–13621
- Syed FA, Modder UIL, Fraser DG, Spelsberg TC, Rosen CJ, Krust A, Chambon P, Jameson JL, Khosla S 2005 Skeletal effects of estrogen are mediated by opposing actions of classical and nonclassical estrogen receptor pathways. *J Bone Miner Res* 20:1992–2001
- Modder UIL, Sanyal A, Kearns AE, Sibonga JD, Nishihara E, Xu J, O'Malley BW, Ritman EL, Riggs BL, Spelsberg TC, Khosla S 2004 Effects of loss of steroid receptor coactivator-1 on the skeletal response to estrogen in mice. *Endocrinology* 145:913–921
- Jorgensen SM, Demirkaya O, Ritman EL 1998 Three-dimensional imaging of vasculature and parenchyma in intact rodent organs with x-ray micro-CT. *Am J Physiol (Heart Circ Physiol)* 275:H1103–H1114
- Bord S, Horner A, Beavan S, Compston J 2001 Estrogen receptors α and β are differentially expressed in developing human bone. *J Clin Endocrinol Metab* 86:2309–2314
- Onoe Y, Miyaura C, Ohta H, Nozawa S, Suda T 1997 Expression of estrogen receptor β in rat bone. *Endocrinology* 138:4509–4512
- McDougall KE, Perry MJ, Gibson RL, Colley SM, Korach KS, Tobias JH 2003 Estrogen receptor- α dependency of estrogen's stimulatory action on cancellous bone formation in male mice. *Endocrinology* 144:1994–1999
- Mohan S, Richman C, Guo R, Amaar Y, Donahue LR, Wergedal J, Baylink DJ 2003 Insulin-like growth factor regulates peak bone mineral density in mice by both growth hormone-dependent and -independent mechanisms. *Endocrinology* 144:929–936
- Kasukawa Y, Baylink DJ, Wergedal JE, Amaar Y, Srivastava AK, Guo R, Mohan S 2003 Lack of insulin-like growth factor I exaggerates the effect of calcium deficiency on bone accretion in mice. *Endocrinology* 144:4682–4689
- Yakar S, Rosen CJ, Beamer WG, Ackert-Bicknell CL, Wu Y, Liu J-L, Ooi GT, Setser J, Frystyk J, Boisclair YR, LeRoith D 2002 Circulating levels of IGF-I directly regulate bone growth and density. *J Clin Invest* 110:771–781
- Kaplan SA 2001 Somatomedin hypothesis: time for reexamination. *Endocrinologist* 11:470–473
- Yakar S, Liu J-L, Stannard B, Butler A, Accili D, Sauer B, LeRoith D 1999 Normal growth and development in the absence of hepatic insulin-like growth factor I. *Proc Natl Acad Sci USA* 96:7324–7329
- Parikka V, Peng Z-Q, Hentunen TA, Risteli J, Elo T, Vaananen HK, Harkonen P 2005 Estrogen responsiveness of bone formation *in vitro* and altered bone phenotype in aged estrogen receptor- α -deficient male and female mice. *Eur J Endocrinol* 152:301–314

Endocrinology is published monthly by The Endocrine Society (<http://www.endo-society.org>), the foremost professional society serving the endocrine community.